

## The use of aeration for arch and pipe collapse in the discharge of cohesive powders from a silo

A. Cannavacciuolo<sup>1)</sup>, D. Barletta<sup>1)</sup>, G. Donsi<sup>1)</sup>, G. Ferrari<sup>1)</sup>, J. Schwedes<sup>2)</sup> and M. Poletto<sup>1)</sup>

<sup>1)</sup> Dipartimento di Ingegneria Chimica e Alimentare, Università di Salerno, Via Ponte don Melillo, 84084 Fisciano (SA), Italy

<sup>2)</sup> Institute for Particle Technology, Technical University of Braunschweig, Volkmaroder Straße 5, 38104 Braunschweig, Germany

Arching and piping can occur during silo discharge of cohesive powders. This happens in general when the outlet size is too small. To achieve proper flow of cohesive materials flow aid devices, such as aeration pads are commonly used in industry. No design criteria, however, are presently available for such kind of devices and, in particular, for the intensity of aeration to be used to avoid such phenomena. Aim of this work is the evaluation of the limiting aeration conditions to produce the collapse of established arches and pipes. Experimental tests are carried out in an aerated flat bottom silo. A simple model is proposed to assess on the prevailing physical phenomena.

### 1 Introduction

Fine and cohesive powders may discharge with some difficulty from silos and hoppers. With these powders, in fact, flow obstructions such as arches and pipes can occur. Jenike (1961 and 1964) proposed design methods to predict the minimum diameter of the silo outlet to avoid arching and piping in gravity flow. According to this approach, when the arch is on the verge of collapsing, its weight is just balanced by the vertical component of the maximum normal stress at the wall. From the force balance on the arch Jenike derived the following equation to determine the critical outlet diameter,  $D$ , that is the smallest outlet diameter to avoid arching

$$D = \frac{\sigma_c \cdot H(\theta)}{\gamma} \quad (1)$$

where  $\sigma_c$  is the material unconfined yield strength,  $\gamma$  is the mass force per unit volume and  $H(\theta)$  is a function of hopper half-angle  $\theta$ , taking into account the geometry of the hypothesized arch. Under gravity flow

$$\gamma = \rho_b g \quad (2)$$

where  $\rho_b$  is the powder bulk density and  $g$  the acceleration due to gravity. For the pipe stability, a similar but more complex approach, due to the different statics of the system, was proposed by Jenike (1961 and 1964).

To avoid arching and piping it is often necessary to provide silos with very large, industrially unacceptable outlets for very cohesive bulk materials. In these cases, additional discharge aids can be fitted to promote flow. Aeration pads are commonly used in the industry to achieve proper flow of cohesive materials. The main effect of aeration is to determine favourable pressure gradients near the hopper outlet. This paper aims at verifying the effectiveness of aeration to determine the collapse of flow obstructions such as domes and pipes. Moreover, the possibility of extending the Jenike approach by correcting the total mass force with the contribution due to the local gas pressure gradients is assessed in the case of arch collapse.

## 2 Experimental set-up

A sketch of the aerated silo used in the experimental tests is reported in Figure 1. The flat bottomed silo has cylindrical walls 3 mm thick, made of transparent Perspex. It is 520 mm high and the internal diameter is 136 mm. At the bottom the silo is provided with a gas distributor made of a sintered brass plate. Different outlet orifices of 22 mm and 33 mm ID can be mounted at the gas distributor level. Further details of the experimental apparatus are given in Donsi *et al.* (2003).

Two different materials were used: a calcium carbonate and a titanium dioxide powder, whose properties are summarized in Table 1. The median of the particle size distribution,  $d_p$ , the bulk density,  $\rho_b$ , the gas permeability,  $k$ , and the lowest gas superficial velocity at which the material rise as a plug in the fluidization column,  $U_p$ , are all reported.

Table 1 Material properties.

Material	Calcium carbonate	Titanium dioxide
$d_p$ [ $\mu\text{m}$ ]	6.68	-
$\rho_b$ [ $\text{kg m}^{-3}$ ]	350	785
$k$ [ $10^9 \text{ m}^2$ ]	6.22	31.50
$U_p$ [ $10^{-3} \text{ m s}^{-1}$ ]	60	19
Geldart group	C	C

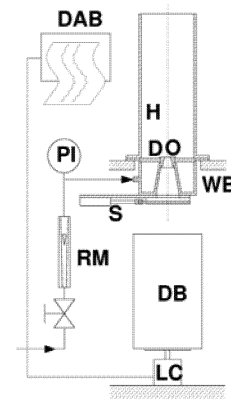


Figure 1 Experimental apparatus: D, gas distributor; DAB, data acquisition board; DB, discharge bin; H, bin; LC, load cell; O, outlet orifice; PI, pressure indicator; RM, rotametre; S, slide lock; WB, wind-box.

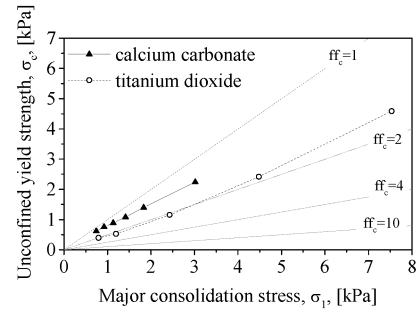


Figure 2 Flow functions of the bulk materials.

The flow properties of the bulk solids were measured in a Schulze ring shear tester. The flow functions are reported in Figure 2.

The fluidization tests were carried out in a 50 mm ID glass column. As an example the fluidization curves of the calcium carbonate is reported in Figure 3. The bed height,  $H_{fb}$ , and the relative bed pressure drop are plotted as a function of the gas superficial velocity,  $U_{fb}$ . The relative pressure drop is calculated as the ratio between the pressure drop in the bed and the weight of the bed per unit of transversal surface area of the fluidization column.

When the pressure drop was equal to the bed weight, a plug formed and moved upwards within the column. When this happened, the plug had to be broken to keep the material inside the column and, therefore, the powder rearranged at the bed bottom. The powder clearly showed aggregation and the permeability of the bed changed. It was therefore possible to further increase the aeration rate until a new plug started to rise. This behaviour appears as a saw toothed pressure drop curve (Figure 3) and shows that every time the plug collapsed, the powder rearranged in a looser structure of aggregates.

The silo was loaded using a funnel. Because of the marked tendency of all powders to aggregate, fresh material was used for each test. The air feeding was started and stepwisely increased after the outlet slide opening.

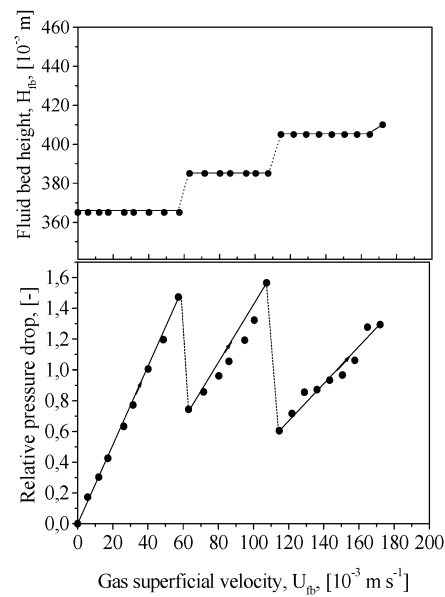


Figure 3 Fluidization curve of calcium carbonate powder.

### 3 Results

Results of discharge experiments for calcium carbonate powder are reported in Figure 4. At the slide opening no discharge occurred because the orifice diameter was too small to have flowing material without aeration. The aeration rate was increased slowly and constantly between set values. At low aeration rates some material discharged leaving a dome close to the orifice. The height of the dome,  $h_d$ , was measured by means of a calliper and its breadth,  $D_d$ , estimated from the mass of the discharged material. The sizes of the dome increased when increasing the aeration rate. An aeration velocity at the distributor of about  $37 \text{ mm s}^{-1}$  was measured to be the critical value for no arching powder flow. Using this aeration procedure no pipe formed at any aeration rate. Sometimes, the formation of very large aggregates of material obstructing the orifice or of small channels did not allow the complete discharge of the silo.

The diagram of the mass of the discharged titanium dioxide at different air superficial velocity is reported in Figure 5.

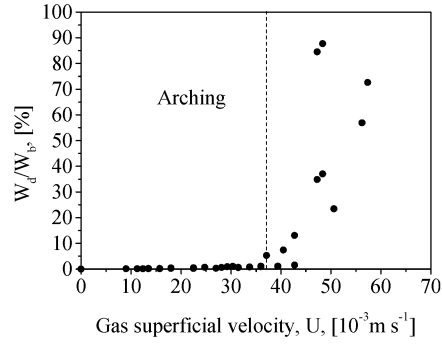


Figure 4 Fraction of calcium carbonate discharged as a function of the aeration rate.

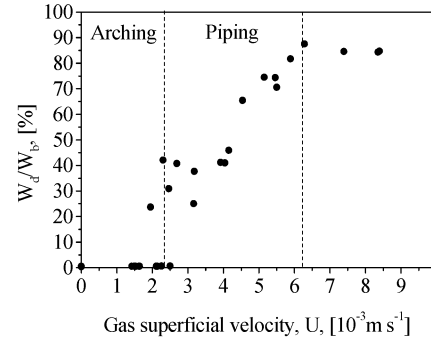


Figure 5 Fraction of titanium dioxide discharged as a function of the aeration rate.

Even with opened silo's outlet, at aeration rate lower than  $2.2 \text{ mm s}^{-1}$  the titanium dioxide was not discharged because an arch formed in proximity of the outlet. At aeration rates between  $2.2 \text{ mm s}^{-1}$  and  $6.3 \text{ mm s}^{-1}$  the arch collapsed but the bin content was only partially discharged because the material formed a vertical pipe having a diameter slightly larger than the outlet. In this range of gas superficial velocities, the higher the aeration rate, the lower was the depth of the pipe and the larger its diameter. The tallest stable pipe was recorded with a bed about  $0.35 \text{ m}$  high. At aeration rates larger than  $6.3 \text{ mm s}^{-1}$  the bin was completely emptied with the exception of a small quantity of material that was left as a cone at the bottom with an angle of repose of about  $40^\circ$ .

#### 4 Discussion

In order to describe the different shapes and sizes of the dome at equilibrium at a certain aeration rate, the total mass force appearing in equations (1) and (3), promoting the arch and pipe collapse and producing the powder consolidation is assumed to be the sum of the weight of the bulk material and of the force due to the interstitial air pressure gradient. This effective body force,  $\gamma^*$ , is therefore given by

$$\gamma^* = \rho_b g + \left. \frac{\partial p}{\partial r} \right|_d \quad (3)$$

where,  $\rho_b$  is the powder bulk density,  $g$  the acceleration due to gravity,  $p$  the gas pressure,  $r$  the distance to the ideal vertex of the conical domain formed by the solids flow, and the subscript 'd' to the derivative indicates that it has to be evaluated at the dome surface. In the case of dome formation an estimate of the local gas pressure gradient at the dome is

$$\left. \frac{\partial p}{\partial r} \right|_d = n\mu \cdot k \cdot U_d \quad (4)$$

Table 2 Values of the unconfined yield strength,  $\sigma_c$ , bulk density,  $\rho_b$ , effective angle of friction,  $\delta$ , and value of the function  $H(\theta^*)$ .

Material	$\sigma_c$ Pa	$\rho_b$ kg m <sup>-3</sup>	$\delta$	$\theta^*$	$H(\theta^*)$ -
Calcium carbonate	410	350	67.5°	12°	2.2
Titanium dioxide	300	740	51.0°	10°	2.2

Equation 4 describes the pressure gradient (positive in the silo inward direction) calculated from the gas pressure drop through the powder, considered as a porous medium. It is as a function of the bed permeability,  $k$ , the local gas velocity,  $U_d$  (positive in the outward direction), the gas viscosity,  $\mu$ , and a dimensionless proportionality constant,  $n$ , which accounts for non

uniformity in the gas velocity distribution on the dome surface. The exit through the orifice at the silo bottom is a preferential pathway for the gas injected through the distributor at the silo bottom. Therefore the gas flow percolating the material to the silo top is relatively small and its contribution to the gas mass balance can be neglected (Donsì *et al.*, 2004). With this simplifying assumption, it is possible to write

$$U_d = \frac{Q}{\Sigma_d} \quad (5)$$

where  $Q$  is the air flow rate fed into the silo and  $\Sigma_d$  is the dome surface area that can roughly be estimated as

$$\Sigma_d = \pi D_d h_d \quad (6)$$

where  $D_d$  is the dome diameter and  $h_d$  its height.

Use of equation 4 requires the powder permeability parameter  $k$ . This was estimated starting from the pressure drop data collected from the fluidization curve at aeration rates below the critical value at which a plug formed in the fluidization column under laminar flow hypothesis

$$k = \frac{\Delta p_{fb}}{H_{fb}} \left/ (U_{fb} \mu) \right. \quad (7)$$

To evaluate the powder consolidation, equation (1) was used with  $\gamma^*$  in place of  $\gamma$

$$\gamma^* = \frac{H(\theta) \cdot \sigma_c}{D_d} \quad (8)$$

The value of  $\gamma^*$  obtained from equation (8) was used to evaluate  $n$  combining equations (3) to (6)

$$n = (\gamma^* - \rho_b g) \frac{\pi D_d h_d}{\mu k Q} \quad (9)$$

The flow factor  $ff_a$  necessary to evaluate  $\sigma_c$  in equation (8) was selected using the appropriate table proposed by Jenike (1964). To this purpose the slope of the channel,  $\theta^*$ , formed inside the bin during the material discharge was supposed to be equal to the cone slope of the funnel after the arch collapse. The values used for  $\theta^*$  are reported in Table 2. A passive state of stresses was also assumed. The unconfined yield strength  $\sigma_c$  and the corresponding major consolidation stress  $\sigma_1$  are obtained from the intersection of the flow factor line and the flow function curve on a  $\sigma_c$ - $\sigma_1$  graph. From the value of  $\sigma_1$  also the bulk density,  $\rho_b$ , and the effective angle of friction,  $\delta$ , were determined. Also these values are reported in Table 2.

Table 3 reports the experimental values of the measured variables at the critical aeration for the arch collapse: the aeration flow rate,  $Q_c$ , the dome height,  $h_d$ , and diameter,  $D_d$ , and the resulting values of  $n$ . The average value of  $n$  for calcium carbonate is about 1.8. The average value of  $n$  for titanium dioxide is about 0.98. The soundness of the physical approach followed in describing the effect of aeration through the combination of the gas pressure gradient with the gravity seems to be confirmed by the values of  $n$  obtained which are of the order of unity.

Table 3 Aeration flow rate,  $Q_c$ , dome height,  $h_d$ , and diameter,  $D_d$ , and dimensionless parameter  $n$  at arch collapse.

Material	$Q_c$ $10^{-3} \text{ m}^3 \text{ s}^{-1}$	$h_d$ $10^{-3} \text{ m}$	$D_d$ $10^{-3} \text{ m}$	$n$ -
Calcium carbonate	0.583	57	50	1.74
	0.583	55	35	1.81
	0.597	70	55	1.76
	0.625	65	55	1.80
	0.022	25	25	1.13
Titanium dioxide	0.033	30	26	1.13
	0.036	25	25	0.86
	0.031	25	25	1.03
	0.043	26	26	0.76
	0.026	25	25	1.19
	0.043	25	25	0.73

## 5 Conclusions

Aeration can significantly affect the discharge of a cohesive powder and, in particular it can avoid the formation of flow impediments like arches and pipes. A modified approach of the original Jenike (1961) method for calculating the critical diameter for the arch collapse procedure was developed by assuming the contribution of the local gas pressure gradient to the total mass force. Experimental results provide some evidence of the correctness of this approach. The extension of this approach to pipe collapse criteria is the object of further studies. First successful tests have been performed and the results compared with the theoretical method to predict the critical pipe diameter. However more tests are necessary to confirm our predicting method.

## 6 References

- Jenike, A.W., 1961, *Gravity flow of bulk solids*. University of Utah, Bulletin 108.
- Jenike, A.W., 1964, *Storage and flow of solids*. University of Utah, Bulletin 123.
- Donsì, G., G. Ferrari, M. Poletto, and P. Russo, 2003, *Kona J.*, 21, 54.
- Donsì, G., G. Ferrari, M. Poletto, and P. Russo, 2004, *Chem. Eng. Res. Des.*, 82, 72.